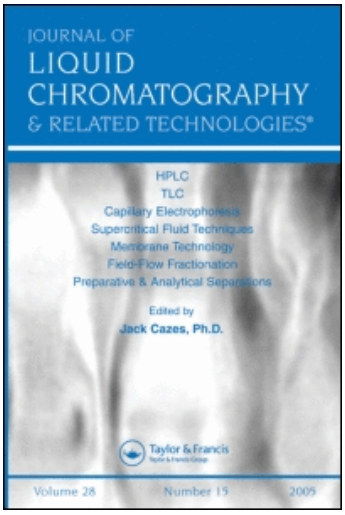

Journal of Liquid Chromatography & Related Technologies

Publication details, including instructions for authors and subscription information:
http://www.informaworld.com/smpp/title~content=t713597273

Data Interpretation for Coupled Molecular Weight Sensitive Detectors in Sec: Interdetector Transport Time

Paul Cheung[a]; Stephen T. Balke[a]; Thomas H. Mourey[b]
[a] Department of Chemical Engineering and Applied Chemistry, University of Toronto, Toronto, Ontario, Canada [b] Research Laboratories B-82, Eastman Kodak Company, Rochester, New York

To cite this Article Cheung, Paul , Balke, Stephen T. and Mourey, Thomas H.(1992) 'Data Interpretation for Coupled Molecular Weight Sensitive Detectors in Sec: Interdetector Transport Time', Journal of Liquid Chromatography & Related Technologies, 15: 1, 39 — 69
To link to this Article: DOI: 10.1080/10826079208018808
URL: http://dx.doi.org/10.1080/10826079208018808

JOURNAL OF LIQUID CHROMATOGRAPHY, 15(1), 39-69 (1992)

DATA INTERPRETATION FOR COUPLED MOLECULAR WEIGHT SENSITIVE DETECTORS IN SEC: INTERDETECTOR TRANSPORT TIME

PAUL CHEUNG[1], STEPHEN T. BALKE[1]*,
AND THOMAS H. MOUREY[2]
[1]*Department of Chemical Engineering and Applied Chemistry*
University of Toronto
Toronto, Ontario, Canada M5S 1A4
[2]*Research Laboratories B-82*
Eastman Kodak Company
Rochester, New York 14650-2136

ABSTRACT

The time required for polymer molecules to pass from one detector to another is a critical parameter for interpretation of multidetector size exclusion chromatography data. A method of utilizing numerical optimization to determine this quantity is presented. The chromatography system included a differential refractive index detector (DRI) in combination with a low-angle laser light scattering photometer (LALLS) and a differential viscometer (DV). The optimization method requires a conventional calibration curve (in terms of intrinsic viscosity rather than molecular weight if the DV detector is used) and the raw data from analysis of a broad molecular weight distribution linear homopolymer standard. A cubic polynomial and a least square cubic spline were used to fit the conventional calibration curve. In interpretation of the DV data, it was necessary to use a least square cubic spline to fit the conventional calibration curve. Results obtained are "effective" in that they intrinsically

* Author to whom correspondence should be addressed.

provide agreement with various molecular weight measures of the standard. Some evidence shows that they are slightly lower than estimates from experimental methods available.

INTRODUCTION

This paper examines data interpretation for a size exclusion chromatography system which includes three detectors: a low-angle laser light scattering photometer (LALLS), a differential viscometer (DV) and a differential refractometer (DRI). In such a system, there are many data interpretation options: resolution correction, allowance for differing detector sensitivities and concentration correction, for example. The paper focuses upon a component of the interpretation, which is even more fundamental than these considerations: the time required for polymer molecules to travel from one detector to another (interdetector transport time). In the next section, the dependence of interdetector transport time on eluent flow rate as well as calculation of weight average molecular weight and intrinsic viscosity are shown. Then, the numerical method to be used here for determining interdetector transport time is described.

THEORY

Split Flow System

Figure 1 shows a schematic of the arrangement of detectors used in this study. The flow is split approximately equally between the LALLS and DRI on one side and the DV on the other. The advantage in this arrangement is that band spreading in the DV is not added to the band spreading in the other two detectors. However, the band spreading in the DRI output does have a contribution from the LALLS.

In a split-flow system, it is necessary to carefully define what is meant by retention time, detection time, interdetector transport time and retention volume. Our definitions are as follows:

Retention time for a particular molecular size is the time required for an eluting molecule of that size to arrive at the DRI.

Detection time for a particular molecular size is the time at which an eluting molecule of that molecular size is detected at a particular detector. For the refractometer, detection time is equal to retention time for a specific molecular size. For the other detectors, there is a time difference, the interdetector transport time, $t_{DRI\text{-}DET}$. Therefore,

$$t_{DRI\text{-}DET} = t_{DRI} - t_{DET} \tag{1}$$

where t_{DRI} and t_{DET} are detection times.

Retention volume, v, for a particular molecular size is the volume of mobile phase which has passed through the columns at the retention time. The property measured at the ith-specific value of v is indicated by the subscript i.

The interdetector transport time between the LALLS and the DRI, based on the physical volumes of the connecting tubing, is given by:

$$t_{DRI\text{-}LALLS} = \frac{V_{DRI}}{Q_{DRI}} - \frac{V_{LALLS}}{Q_{LALLS}} \tag{2}$$

where V_{DRI} and V_{LALLS} are the mobile phase volumes measured from the point at which the flow is split to the DRI and LALLS respectively, Q_{DRI} and Q_{LALLS} are the volumetric flow rate passing through the DRI and LALLS respectively. Since DRI and LALLS are on the same branch of the outlet line in our system, Q_{DRI} must be equal to Q_{LALLS}.

Similarly, the interdetector transport time between the DV and the DRI is given by:

$$t_{DRI\text{-}DV} = \frac{V_{DRI}}{Q_{DRI}} - \frac{V_{DV}}{Q_{DV}} \qquad (3)$$

where V_{DRI} and V_{DV} are the mobile phase volumes measured from the point at which the flow is split to the DRI and DV respectively, Q_{DRI} and Q_{DV} are the volumetric flow rate passing through the DRI and DV respectively.

If desired, the interdetector transport time can be converted into an interdetector volume value if the split of flow is known or assumed. However, this interdetector volume is not necessarily equal to the physical volume between detectors (1,2).

From Equations (2) and (3), it can be seen that a change in the flow rate of each individual branch without a change in the total flow rate will affect both $t_{DRI\text{-}LALLS}$ and $t_{DRI\text{-}DV}$. However, such a change will not affect the ratio of detection volume increment to detection time increment for data collected in each chromatogram. The increment referred to is the distance between consecutive data points expressed as either detection volume or detection time. The ratio is therefore always equal to the total flow rate, Q. Also, chromatogram shape and breadth are unaffected by changes in the split (assuming no difference in axial dispersion effects in each branch).

Equations for Whole Polymer $\bar{M}_w$ and $[\bar{\eta}]$

Whole polymer $\bar{M}_w$ and whole polymer $[\bar{\eta}]$, calculated from LALLS and DV respectively, are not affected by the interdetector transport time nor by the flow split. Even a variation of the split during a run will not affect their values so long as Q is constant.

The whole polymer weight average molecular weight is calculated from the LALLS output, assuming the product of the second virial coefficient and concentration is negligible, using:

$$\bar{M}_w = \frac{\Delta v_{LALLS} \; \Sigma R_\theta}{m_{LALLS} \quad K} \tag{4}$$

where $\Delta v_{LALLS} = Q_{LALLS} \Delta t_{LALLS}$ and Δt_{LALLS} is the detection time increment for data collected for the LALLS, R_θ is the excess Rayleigh scattering measured by LALLS at each detection time and Σ represents the summation over the total detection time, K is the LALLS's optical constant, and m_{LALLS} is the total mass of polymer which has passed through the LALLS in a run.

Two methods are used here to calculate the whole polymer intrinsic viscosity. The first utilizes only the area under the DV output and the total mass of polymer passing through the DV in a run, m_{DV}:

$$[\bar{\eta}] = \frac{\Delta v_{DV} \; \Sigma \eta_{sp}}{m_{DV}} \tag{5}$$

where $\Delta v_{DV} = Q_{DV} \Delta t_{DV}$ and Δt_{DV} is the detection time increment for data collected for the DV and η_{sp} is specific viscosity measured by the DV.

The second method uses the DRI output along with the narrow standard calibration for intrinsic viscosity:

$$[\bar{\eta}] = \Delta v \; \Sigma W_N [\eta]_{cal} \tag{6}$$

where $\Delta v = Q \Delta t_{DRI}$ and Δt_{DRI} is the detection time increment for data collected for the DRI, W_N is the normalized DRI response at each detection time and $[\eta]_{cal}$ is the intrinsic viscosity obtained from the narrow standard calibration at that time.

Equations for Local Values of Polymer Properties

Local values are the property values of the molecules at a particular retention volume. They are affected by the interdetector transport time and hence are affected by the flow split. The reason for this is that in order to calculate local weight average molecular weight, $\bar{M}_{w,i}$ or local intrinsic viscosity, $[\bar{\eta}]_i$, the output from the LALLS or DV detectors must be superimposed on the output from the DRI detector to obtain corresponding concentration values, c_i, of polymer in the eluent at that ith-specific retention volume. The quantity c_i is also a function of Q as well. The accuracy of this superposition depends upon the accuracy of the interdetector transport time. Once this transport time has been determined, the local values as measured by LALLS and DV can be calculated as a function of retention volume for all samples.

$\bar{M}_{w,i}$ is calculated from the LALLS and DRI output using:

$$\bar{M}_{w,i} = \frac{R_{\theta,i}}{K\ c_i} \tag{7}$$

$[\bar{\eta}]_i$ is calculated from the DV and DRI output using:

$$[\bar{\eta}]_i = \frac{\eta_{sp,i}}{c_i} \tag{8}$$

Total Flow Rate

Based on the equations described above, both the accuracy and precision of the total flow rate affect all calculated values. Interestingly, absolute accuracy and short term random fluctuation are of secondary

importance. Systematic long term fluctuation causes the most serious problem. In particular, if Q varies systematically from injection to injection, then the total retention volume will vary. This affects two aspects of the results:

i) plots of local property values versus retention volume.

In a plot of local property values, such as the logarithm of molecular weight (M_i) or intrinsic viscosity ($[\bar{\eta}]_i$) at a particular retention volume versus retention volume, the conventional calibration curve, will be affected. Effects of flow rate on this curve are well known and can be very significant for steep curves (modern high resolution columns). The universal calibration curve, a plot of hydrodynamic volume, expressed as $[\bar{\eta}]M$, versus retention volume, will be similarly influenced.

ii) the detection volume increment value, Δv_{DET}, will vary, affecting the calculated concentrations, c_i.

Calculations of $\bar{M}_w$ and $\bar{M}_{w,i}$ from LALLS as well as $[\bar{\eta}]$ and $[\bar{\eta}]_i$ from DV depend upon accurate Δv_{DET} values. However, this source of error is of secondary importance. It can readily be shown that a 1% inaccuracy in flow rate can cause a 1% inaccuracy in Δv_{DET}, which will result in a corresponding 1% inaccuracy in both the whole and local property values.

It is possible for both of the above aspects to be present. For example, a plot of log $\bar{M}_{w,i}$ versus retention volume is very sensitive to variations in total flow rate because both are present. In contrast, whole polymer properties calculated from Equations (4) and (5) are much less affected by variations of total flow rate, since they are affected only by the second mentioned aspect.

The average flow rate over a run can be obtained by the collection and measurement of the eluent leaving the size exclusion chromatograph (SEC). An alternative method is to include an internal standard in the run, so that a reference point is available for flow rate correction. A consistent flow rate should also provide the correct molecular weight averages ($\bar{M}_n$, $\bar{M}_w$, $\bar{M}_z$) calculated from the narrow standard calibration. If the flow rates between runs are founded to vary significantly, the variation within runs can be important as

well. However, in order to determine the variation of flow rate during a run, other equipment must be on-line (e.g. a thermal pulse flow meter (3)). Any noticeable change in flow rate should be corrected before the local properties are calculated.

Representation of Narrow Standard Calibration: Cubic Polynomial fit versus Least Square Cubic Spline fit

Before the determination of the transport time, the narrow standard calibration must be well fit by an equation. A cubic polynomial function is commonly used. When it is unable to provide an adequate representation of the calibration curve, a least square cubic spline approach can be used. A cubic spline consists of sections of cubic polynomials whose boundary points are continuous and smooth. The adequacy of the fit can be checked by a plot of the residuals between the fitted curve and the actual data. A random scatter of residual values around zero indicates an unbiased fit. In addition, the calculation of whole polymer properties of a broad standard, such as molecular weight averages and intrinsic viscosity, based on the narrow standard calibration shows accuracy. If the calculated value differs significantly from the "true" values, then possibly the fit is inadequate, the flow rate has changed or the columns have degraded.

Determination of Interdetector Transport Time Given the Correct Total Flow Rate and a Constant Split of Flow

In accordance with usual practice, this paper assumes that the different detector responses can be superimposed by simply using the correct transport time delay to shift one chromatogram over another and no resolution is necessary for a broad standard. No attempt is made to correct for the effect of different cell sizes.

The sensitivity of the local polymer properties to different values of interdetector transport time and flow rate is examined by varying the latter two variables in turn and calculating the resulting local property values as a function of retention volume.

The criteria for the correct interdetector transport time (with the correct total flow rate) are specified as follows:

Log $\bar{M}_{w,i}$ versus v data obtained from applying LALLS and DRI to a broad standard should superimpose upon the conventional calibration curve determined by injecting narrow standards and using DRI to obtain peak retention volumes; log $[\bar{\eta}]_i$ versus v data obtained from applying DV and DRI to a broad standard should superimpose upon the plot of log $[\bar{\eta}]_i$ versus v obtained by injecting narrow standards and using DRI to obtain peak retention volumes. There is now considerable experimental and theoretical justification for expecting this superposition (4,5). In particular, for such broad standards, the results are expected to be independent of resolution correction (4,5). Different size detector cells can be a source of problem, if their effect on the shape of the chromatograms is significant. However, in that case, the whole concept of being able to superimpose data by specifying one value of interdetector volume is in question. Yet another possibility is that differences in the sensitivity of the detectors can result in inaccurate local values ($\bar{M}_{w,i}$ and $[\bar{\eta}]_i$) which, in turn, cause difficulties in accurately applying the criteria (6).

A numerical search method (the Nelder-Mead Simplex Method) is used to determine the optimal interdetector transport time values necessary to satisfy the criteria once the correct flow rate is given. The objective functions used in the search method are contained in Appendix I. Although resolution correction is probably not important in the specific type of interpretation utilized here, as added insurance, certain portions of a chromatogram were selected so that they should be least likely affected by dispersion. In this work, 13 data points around the inflection point (the point of maximum slope) on each side of the DRI chromatogram were used in the objective functions. An additional

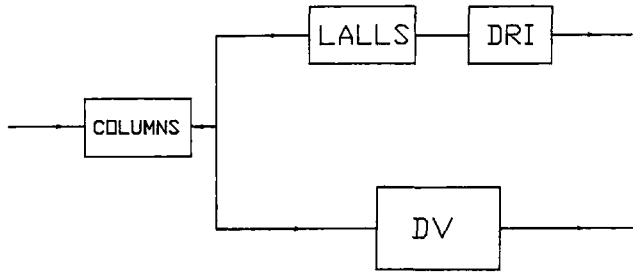

FIGURE 1: A schematic of the multidetector SEC system.

advantage of this selection was that the inflection regions also had a strong signal-to-noise ratio and a high sensitivity toward interdetector transport time.

The sensitivity of the optimal interdetector transport time to the change of total flow rate is examined by varying the "correct" flow rate in the numerical search.

EXPERIMENTAL

A schematic of the instrumentation used is shown in Figure 1. Three 5 μm-particle-diameter 7.5 mm i.d. x 300 mm PLgel mixed-bed columns (Polymer Laboratories, Amherst, MA, U.S.A.) were used. The eluate from the columns was split into two branches. On one branch, the eluate first passed through a KMX-6 LALLS (LDC Analytical, Riviera Beach, FL, U.S.A.) and then through a Waters Model 410 DRI (Waters Associates, Milford, MA, U.S.A.). A Viscotek Model 100 DV (Viscotek, Porter, TX, U.S.A.) was placed on the other branch. The split was made to be 1:1 by adjusting the back pressure of the DV branch. Uninhibited tetrahydrofuran sparged continuously with helium flowed through the columns at a nominal flow rate of 1.0 mL/min. Actual flow rate was measured by collecting the eluate in a calibrated

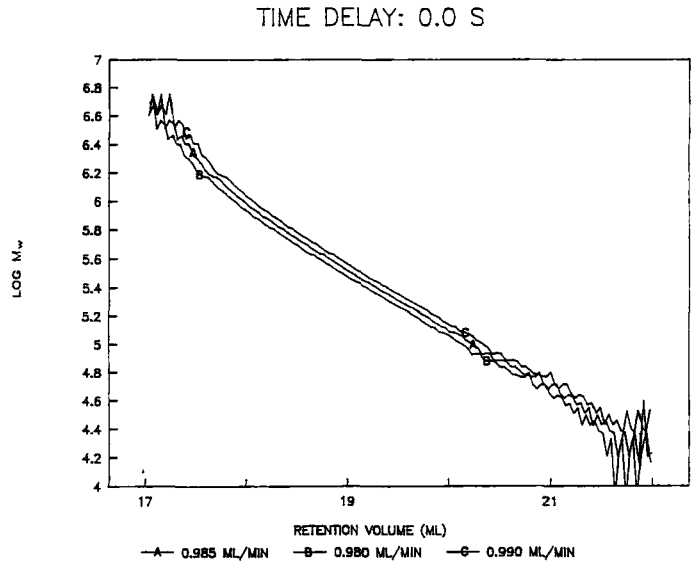

FIGURE 2: The effect of different flow rates on local weight average molecular weight of a broad standard at zero interdetector transport time (time delay).

volumetric flask. For polymer analysis, ten injections, 100 μL each, of the same broad polystyrene standard (NBS 706) sample with a concentration of 1.12 mg/mL were made.

RESULTS AND DISCUSSION

Sensitivity Analysis

The very high sensitivity of local weight average molecular weight values to flow rate and interdetector transport time could be observed in Figures 2 and 3 respectively. These plots of log $\bar{M}_{w,i}$ versus v, obtained from

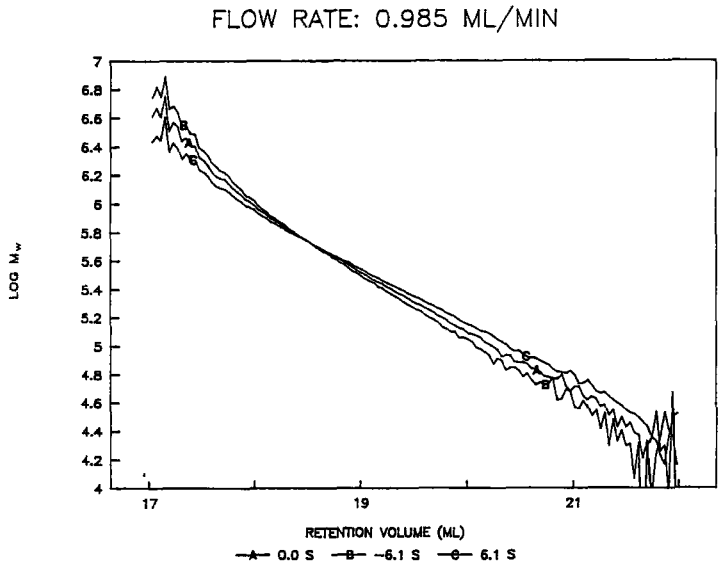

FIGURE 3: The effect of different interdetector transport times on local weight average molecular weight of a broad standard at a flow rate of 0.985 mL/min.

using LALLS and DRI data for the broad standard with different assumed values of flow rate (Figure 2) and with different assumed values of interdetector transport time (Figure 3) are shown. Similar plots could be obtained for log $[\bar{\eta}]_i$ versus v. The change in the flow rate caused the whole curve to shift left or right because the abscissa was being compressed or expanded. The variation of time delay changed the slope of the curve due to different superpositions of the LALLS chromatogram on the DRI chromatogram.

Narrow Standard Calibration

Twenty-eight narrow polystyrene standards were used to prepare the narrow standard calibration. Figures 4 and 5 show the cubic polynomial fits to

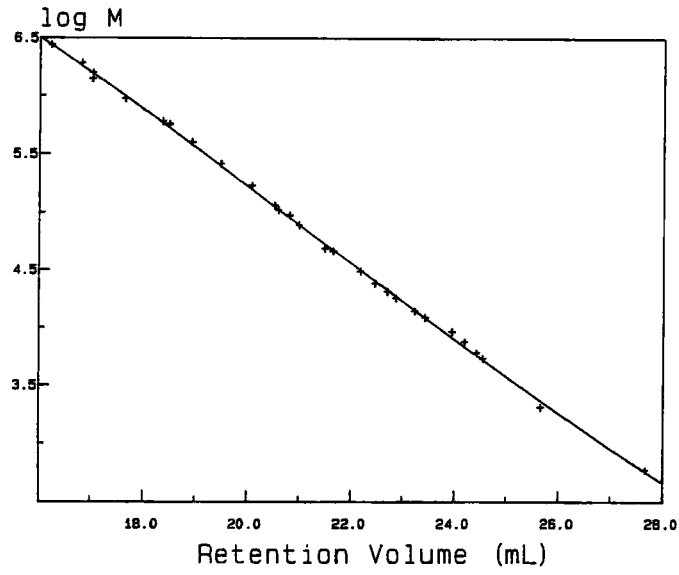

FIGURE 4: The cubic polynomial fit to the molecular weight data for narrow standard calibration.

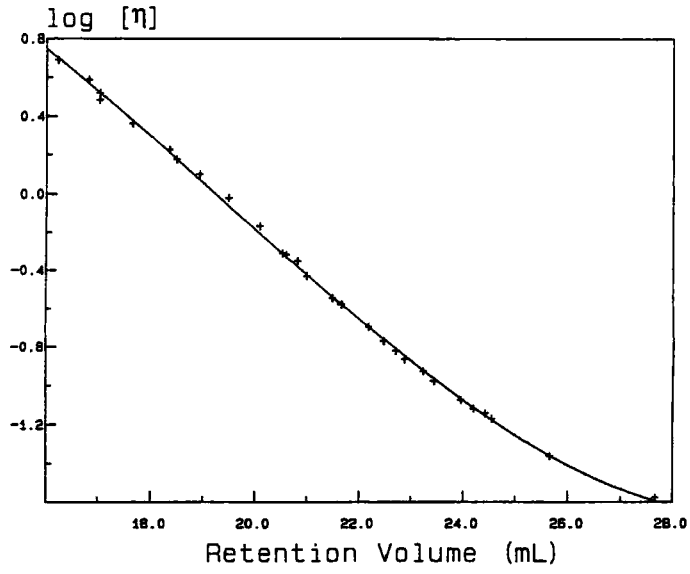

FIGURE 5: The cubic polynomial fit to the intrinsic viscosity data for narrow standard calibration.

log M_i and log $[\bar{\eta}]_i$ versus v data, respectively. Figures 6 and 7 show the corresponding plots of residuals as % error in M_i and $[\bar{\eta}]_i$ versus v, respectively. The residual plots show that the data points oscillated around the polynomial fits in a non-random manner. These oscillations might not be observable if a fewer number of standards was used. Such oscillations have been previously observed and have been founded to be properties of the columns likely associated with irregular packing (7,8). As a comparison, a least square cubic spline was also applied to give calibration curves. The plots of residuals of the spline fits for M_i and $[\bar{\eta}]_i$ in Figures 8 and 9 respectively show the removal of systematic variation and the decrease of deviation by applying the spline fit. In this work, both the cubic polynomial and the least square cubic spline were used in turn to represent the narrow standard calibration in the search for interdetector transport times.

As previously described, the average flow rate during a run was monitored by the measurement of the eluent from the SEC. The actual flow rate was determined to be 0.985 mL/min with a standard deviation of 0.002 mL/min during the narrow standard calibration and the broad standard runs. Although the value was different from the nominal flow rate of 1.0 ml/min, the fluctuation of flow rate, which can cause a greater change in the molecular weight averages calculated from a narrow standard calibration, was insignificant. For the NBS 706 polystyrene standard used, the "true" values and their standard deviations as a percent of the mean were: $\bar{M}_n$, 123200 ± 4.6%; $\bar{M}_w$, 275600 ± 1.7%, $\bar{M}_z$, 434800 ± 2.0% and $[\bar{\eta}]$, 0.94 ± 3%.

Table 1 shows the whole polymer properties obtained for ten runs using narrow standard calibrations. Also shown are the overall averages of the ten runs and their standard deviations. It is evident that most molecular weight averages encompass the true values, no flow rate correction for the fluctuation is necessary for each run. The whole polymer intrinsic viscosity values were calculated using Equation (6) with each of the two fits of the narrow standard calibration for intrinsic viscosity used in turn. The values obtained with the

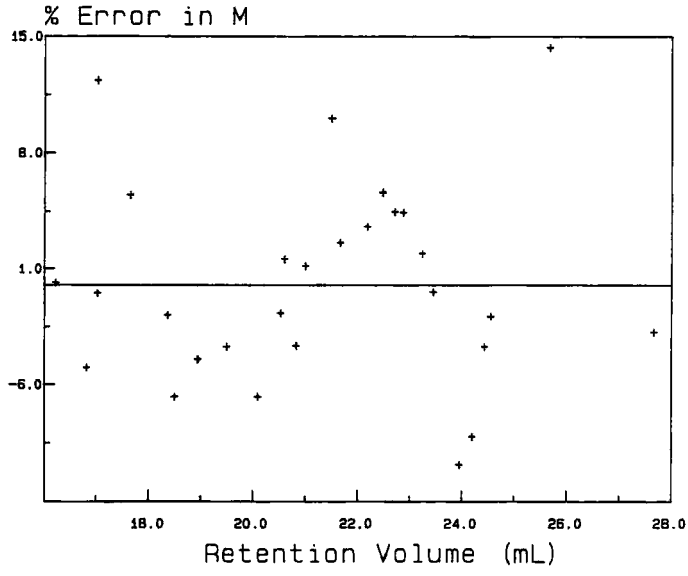

FIGURE 6: The residual plot of the data shown in Figure 4.

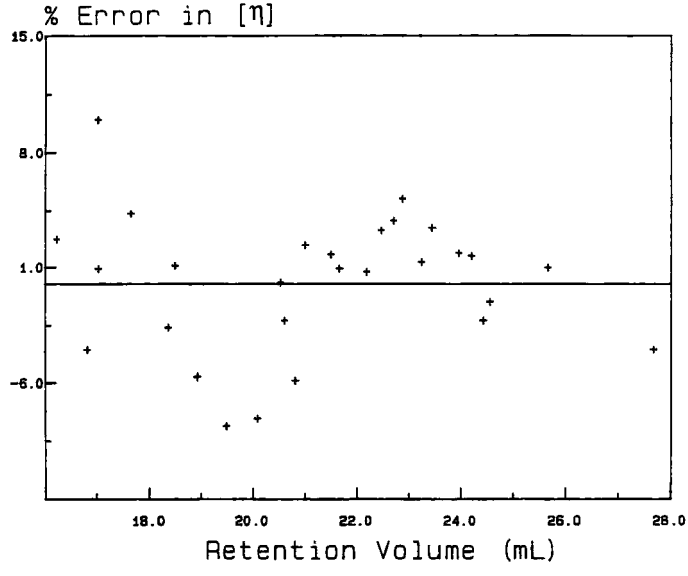

FIGURE 7: The residual plot of the data shown in Figure 5.

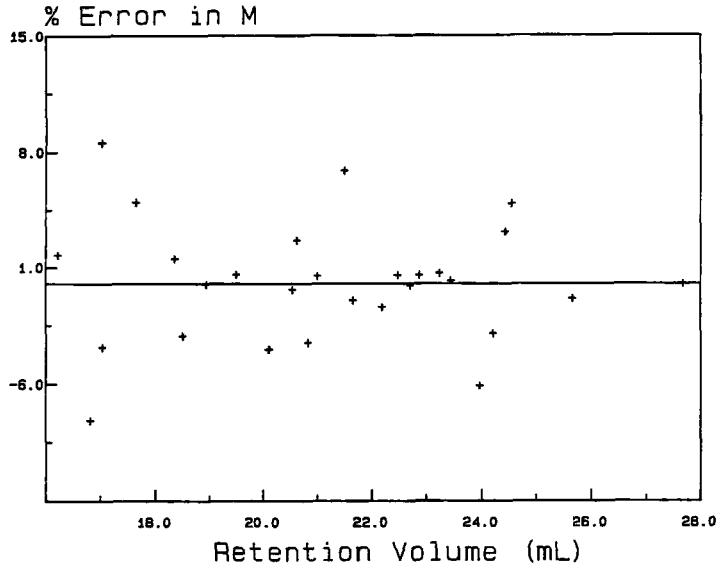

FIGURE 8: The residual plot of the least square cubic spline fit of the molecular weight data for narrow standard calibration.

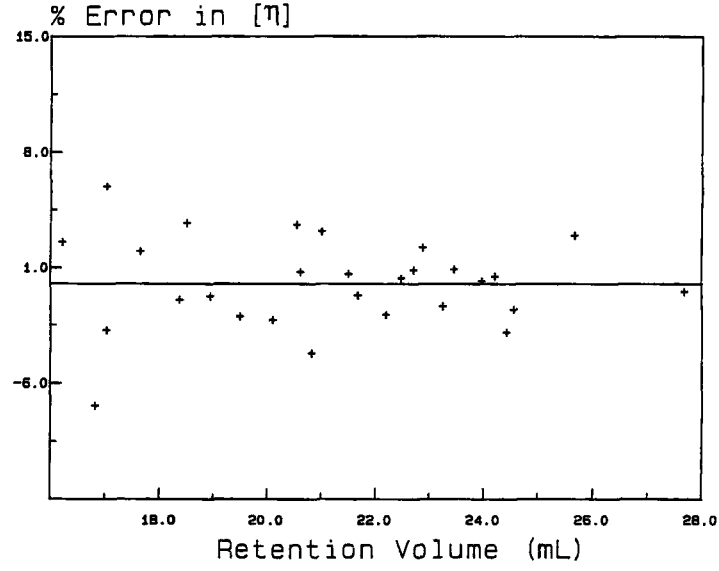

FIGURE 9: The residual plot of the least square cubic spline fit of the intrinsic viscosity data for narrow standard calibration.

TABLE 1

Whole Polymer Properties Measured by the DRI

Narrow Standard Calibration:	Cubic Polynomial $\bar{M}_n$	$\bar{M}_w$	$\bar{M}_z$	$[\bar{\eta}]$ (dL/g)	Least Square Cubic Spline $[\bar{\eta}]$ (dL/g)
True Value:	123200	275600	434800	0.940	0.940
Run No.					
1	116200	273100	441200	0.884	0.918
2	120900	274300	442900	0.883	0.917
3	114900	271900	437000	0.886	0.920
4	124400	273000	434500	0.895	0.930
5	124200	274300	440200	0.883	0.918
6	115500	272900	439900	0.885	0.920
7	120200	273300	439100	0.885	0.919
8	125800	276200	446800	0.880	0.915
9	119800	273100	438700	0.885	0.919
10	121900	274800	444200	0.882	0.917
Average:	120400	273700	440400	0.885	0.919
1σ:	3900	1200	3600	0.004	0.004

cubic polynomial calibration were more than one standard deviation lower than the "true" value. It was attributed to the poor representation of the calibration by cubic polynomial fit as mentioned above. The implementation of the cubic spline fit on intrinsic viscosity gave much better values.

Interdetector Transport Time Determination

In searching for the correct interdetector transport time given the correct total flow rate and a constant split of flow, the objective functions used to

TABLE 2

Interdetector Transport Times Obtained from the Search

Narrow Standard Calibration:	Cubic Polynomial ($\pm 1\sigma$)	Least Square Cubic Spline ($\pm 1\sigma$)
$t_{DRI\text{-}LALLS}$ (s)	14.56 ± 0.55	14.71 ± 0.53
$t_{DRI\text{-}DV}$ (s)	-0.52 ± 0.37	-0.01 ± 0.19

determine when the criteria were satisfied are shown in Appendix I. The error variances of c, R_θ, and η_{sp} were estimated from the ten sets of data. The standard deviation due to the fit of narrow standard calibration was approximated by the cubic polynomial regression. The results of the search are summarized in Table 2. The values shown in the table were the averages of ten runs, along with the standard deviations. Both $t_{DRI\text{-}LALLS}$ and $t_{DRI\text{-}DV}$ did not depend on the choice of narrow standard calibration: a cubic polynomial or a least square cubic spline. However, as will be discussed later, the least square cubic spline calibration gave a better fit to the local intrinsic viscosity data obtained from the search because of the inability of the cubic polynomial to accurately fit the narrow standard data for intrinsic viscosity.

Results of applying different methods along with the standard deviations for determination of $t_{DRI\text{-}LALLS}$ to the same detector system in previous work are shown in Table 3 (9).

The first method in Table 3 utilizes the difference between peak onset or peak time for a narrow standard passing through each detector to determine interdetector volume. The second similarly utilizes a narrow standard of sufficiently high molecular weight to be excluded from all of the pores in the

TABLE 3

Interdetector Transport Time between LALLS and DRI Determined by Several Methods

	Transport Time (s) (± 1σ)
Method 1 (narrow standard)	
peak onset	17.1 ± 0.7
peak maxima	18.9 ± 0.9
Method 2 (excluded narrow standard)	
peak onset	16.3 ± 0.3
peak maxima	19.6 ± 0.3
zero slope	19.5 ± 0.9
Method 3 (no column)	8.7 ± 1.7
Method 4 (numerical optimization)	15.8 ± 0.4
Method 5 (spectrophotometric)	16.1 ± 0.4

packing. The "zero slope" method utilizes the point of zero slope in apparent molecular weight versus retention volume plots at different assumed values of interdetector volume (10). The fourth method in Table 3 is numerical optimization, an earlier version of the method described in this paper. The fifth method mentioned is a new one based upon using the LALLS as a spectrophotometer (9). Table 3 shows that these diverse experimental methods result in diverse values for the interdetector volume. As discussed by Mourey and Miller (9), the best values from experimental methods are likely those determined when peak onset are used rather than peak maxima.

By comparing the results listed in Tables 2 and 3, the interdetector transport time between LALLS and DRI as determined by the search appeared slightly lower than most experimentally values determined at a different date.

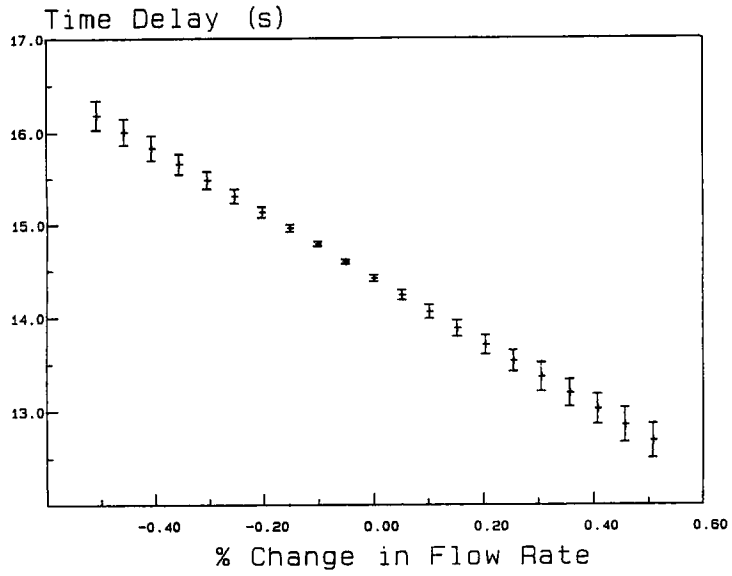

FIGURE 10: The sensitivity of the interdetector transport time between LALLS and DRI to the % change in the flow rate of 0.985 mL/min. The error bar represented 95% confidence interval.

However, the difference of less than two seconds in the transport time corresponds to a difference of less than 0.02 mL in interdetector volume. Since the data of Table 3 were obtained several months earlier than the data of Table 2, this small change may be attributable to changes in the system over that long period of time. In the case of t_{DRI-DV}, no value obtained from other methods is available for comparison with the results of the search.

Figure 10 showed the sensitivity of the interdetector transport time between LALLS and DRI to the percentage change in the flow rate of 0.985 mL/min. Each error bar in the figure represented the 95% confidence interval of time delay between the detectors from the numerical search. The error bar reached a minimum as the flow rate approached the "true" value. This plot demonstrates the importance of flow rate correction.

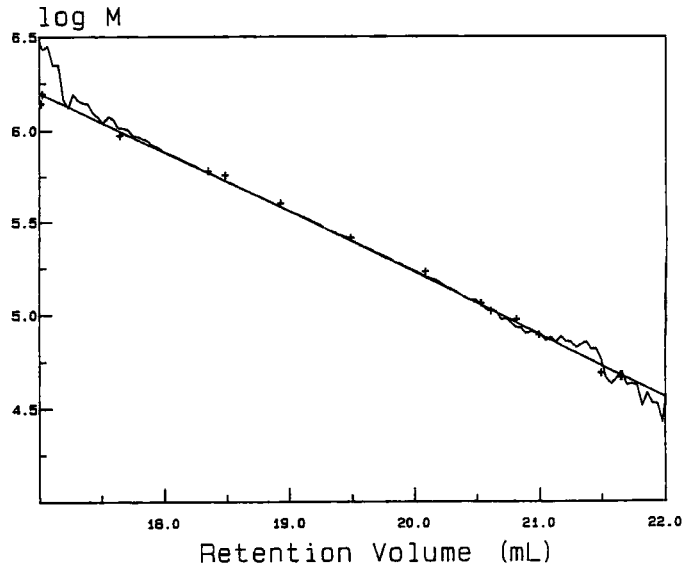

FIGURE 11: The superposition of log $\bar{M}_{w,i}$ of NBS 706 and log $M_{cal,i}$, obtained from the search of the interdetector transport time between LALLS and DRI and the cubic polynomial fit to the data of narrow standards, respectively. The crosses were the narrow standard data.

Figures 11 to 14 showed the superposition of the narrow standard calibration on the curves obtained from the search for two of the runs. In these figures, the smooth curves were either the narrow standard calibrations from the cubic polynomial fit (Figures 11 and 13) or the least square cubic spline fit (Figure 12 and 14); the noisy curves were obtained from the search based upon the chromatograms of a single broad standard. The noisy appearance of the searched curves at both large and small retention volumes was due to the noise in the tails of broad standard chromatograms. The crosses were the actual narrow standard data. The narrow standard data were included in the plots to show the adequacy of all fits to the narrow standard calibrations.

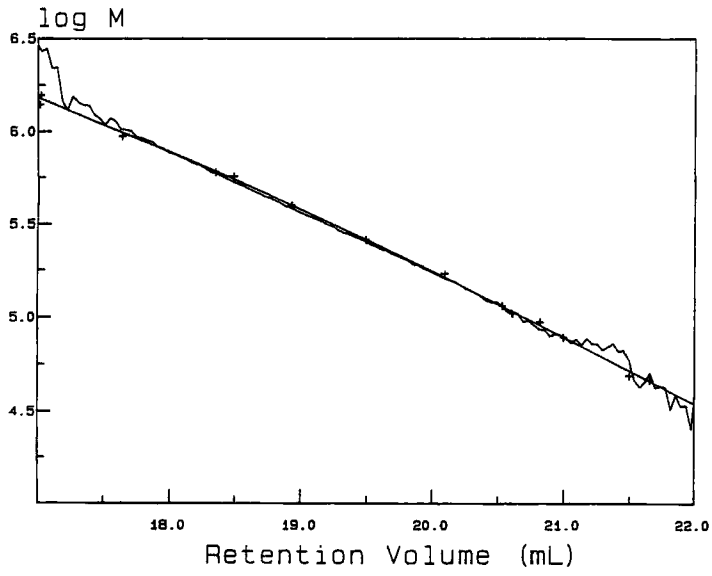

FIGURE 12: The superposition of log $\bar{M}_{w,i}$ of NBS 706 and log $M_{cal,i}$, obtained from the search of the interdetector transport time between LALLS and DRI and the least square cubic spline fit to the data of narrow standards, respectively. The crosses were the narrow standard data.

In the plots of log M versus v, Figures 11 and 12, the superposition of the polynomial fit was superior to that of the spline fit, despite that the spline fit gave a better representation of the narrow standard data. However, the difference in the two fits over the 18 mL to 20 mL region was less than 5% in M and was within the experimental uncertainty. For the same reason, as listed in Table 3, $t_{DRI\text{-}LALLS}$ remained almost unchanged, regardless of which narrow standard calibration fit was used in the search.

In the plots of log $[\bar{\eta}]$ versus v, Figures 13 and 14, the polynomial fit did not give a true picture of the narrow standard data: a 9% error at 19.5 mL was evident. The consequence was that superposition was much improved by

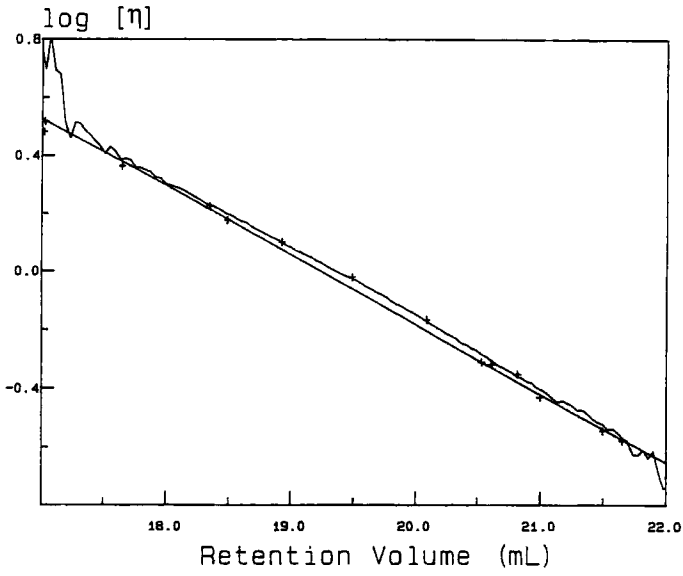

FIGURE 13: The superposition of log $[\bar{\eta}]_i$ of NBS 706 and log $[\eta]_{cal,i}$, obtained from the search of the interdetector transport time between DV and DRI and the cubic polynomial fit to the data of narrow standards, respectively. The crosses were the narrow standard data.

using the spline fit instead of the polynomial fit. For t_{DRI-DV}, the transport time changed from -0.52 s to -0.01 s by replacing the polynomial fit with the spline fit.

CONCLUSIONS

A method of using numerical optimization to obtain an estimate of interdetector transport time was presented. The values so obtained are effective in that they provide correct whole polymer molecular weight averages and intrinsic viscosity as well as superposition of local values of weight average

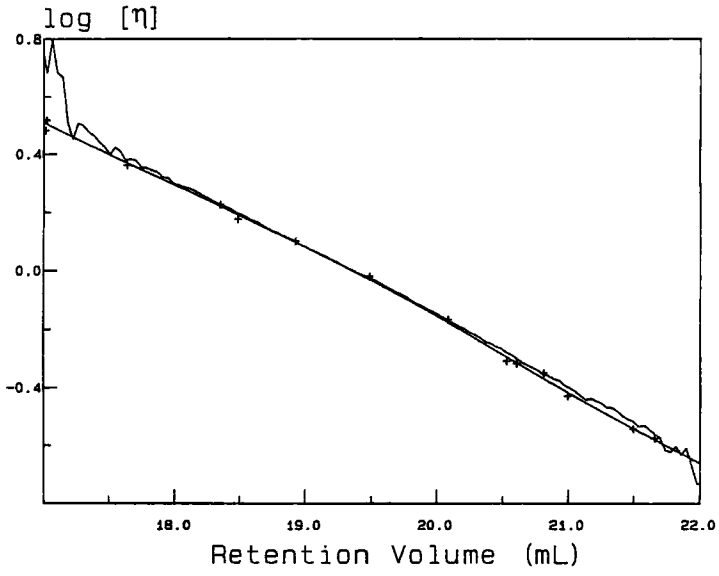

FIGURE 14: The superposition of log $[\bar{\eta}]_i$ of NBS 706 and log $[\eta]_{cal,i}$, obtained from the search of the interdetector transport time between DV and DRI and the least square cubic spline fit to the data of narrow standards, respectively. The crosses were the narrow standard data.

molecular weight and intrinsic viscosity versus retention volume plots upon the respective plots obtained from narrow standards. Some evidence is shown to demonstrate that the values of the interdetector transport time obtained are slightly lower than those from experimental methods.

In implementing the numerical optimization, the choice of a spline fit over a polynomial fit for representing the narrow standard calibration curve provided a significant improvement for the intrinsic viscosity results.

It was also demonstrated that the local molecular weight and intrinsic viscosity values as calculated by LALLS & DRI and DV & DRI respectively

were very sensitive to both flow rate and interdetector transport time. However, no flow rate correction was required for our results.

REFERENCES

1. Bressau, R., "Liquid Chromatography of Polymers and Related Materials II", Cazes, J. and Delamare, X. (Editors), Marcel Dekker, New York, 1980, pp. 73-93.

2. Martin, M., Chromatographia, 15(7), 426(1982).

3. Lew, R., Ho, M. and Balke, S.T., J. Liq. Chromatogr., 13, 453(1990).

4. Styring, M.G., Armonas, J.E. and A.E. Hamielec, A.E., J. Liq. Chromatogr., 10, 783(1987).

5. Hamielec, A.E. and Meyer, H., "Developments in Polymer Characterisation - 5", Dawkins, J.V. (Editor), Elsevier Applied Science, London, 1986, pp. 95-130.

6. Garcia Rubio, L.H., "Detection and Data Analysis in SEC", Provder, T. (Editor), American Chemical Society, Washington D.C., 1987, pp. 220-239.

7. Balke, S.T., Cheung, P., Lew, R. and Mourey, T.H., J. Liq. Chromatogr., 13, 2929(1990).

8. Mourey, T.H., Miller, S.M., and Balke, S.T., J. Liq. Chromatogr., 13, 435(1990).

9. Mourey, T.H. and Miller, S.M., J. Liq. Chromatogr., 13, 693(1990).

10. Lecacheux, D. and Lesec, J., J. Liq. Chromatogr., 5, 2227(1982).

11. O'Driscoll, K.F., Kale, L.T., Garcia Rubio, L.H. and Reilly, P.M., J. Polym. Sci. Poly. Chem. Ed., 22, 2777(1984).

APPENDIX I

Formulation of Objective Functions

A. The determination of interdetector transport time between LALLS and DRI.

In order to match the $\bar{M}_{w,i}$ curve of a broad standard determined by LALLS and DRI with the calibration from the peak retention volumes of narrow standards, we must minimize the function (11):

$$O_1(t_{DRI\text{-}LALLS}) = \sum_{i=1}^{n} \frac{(\bar{M}_{w,i} - M_{cal,i})^2}{s_i^2}$$

where n is the number of data points used in the search.

$\bar{M}_{w,i}$ is the local molecular weight determined by LALLS and DRI at ith-specific retention volume. It is a function of the transport time.

$M_{cal,i}$ is the molecular weight at ith-specific retention volume, obtained from the cubic polynomial or the least square cubic spline fit to narrow standard calibration.

s_i^2 is an estimate of the total error variance at ith-specific retention volume and is used as a weighting factor. In this case, since there is error in both $\bar{M}_{w,i}$ and $M_{cal,i}$, s_i^2 must account for error in both.

Let

$$s_i^2 = s_{LALLS,i}^2 + s_{cal,i}^2$$

where $s_{LALLS,i}^2$ is the error variance estimate associated with $\bar{M}_{w,i}$ and $s_{cal,i}^2$ is the error variance estimate of $M_{cal,i}$.

$s_{cal,i}^2$ is estimated from the linear regression of the polynomial.

$s_{LALLS,i}^2$ is obtained from applying error propagation analysis to the equation:

$$\bar{M}_{w,i} = \frac{R_{\theta,i}}{K\, c_i}$$

Assume no error in K and applying error propagation analysis:

$$s_{LALLS,i}^2 = \left(\frac{\partial \bar{M}_w}{\partial c}\right)_i^2 s_{c_i}^2 + \left(\frac{\partial \bar{M}_w}{\partial R_\theta}\right)_i^2 s_{R_{\theta,i}}^2$$

where

$$\frac{\partial \bar{M}_{w,i}}{\partial c_i} = \frac{\bar{M}_{w,i}}{c_i}$$

$$\frac{\partial \bar{M}_{w,i}}{\partial R_{\theta,i}} = \frac{1}{K\, c_i}$$

s_{Ci}^2 is the error variance estimate associated with c_i, the concentration of polymer in the eluent at retention volume i, and $s_{R\theta,i}^2$ is the error variance estimate of $R_{\theta,i}$ measured by LALLS at ith-specific retention volume.

B. The determination of interdetector transport time between DV and DRI.

In an exactly similar manner to that in part A above, we have the following objective function to be minimized for the determination of $t_{DRI\text{-}DV}$:

$$O_2(t_{DRI\text{-}DV}) = \sum_{i=1}^{n} \left(\frac{\left[\bar{\eta}\right]_{DV,i} - \left[\eta\right]_{cal,i})^2}{\left(\frac{\partial [\bar{\eta}]_{DV}}{\partial c} s_c\right)_i^2 + \left(\frac{\partial [\bar{\eta}]_{DV}}{\partial \eta_{sp}} s_{\eta_{sp}}\right)_i^2 + (s_{[\eta]_{cal}})_i^2} \right)$$

where

$$\frac{\partial[\bar{\eta}]_{DV,i}}{\partial c_i} = \frac{[\bar{\eta}]_{DV,i}}{c_i}$$

$$\frac{\partial[\bar{\eta}]_{DV,i}}{\partial \eta_{sp,i}} = \frac{1}{c_i}$$

n is the number of data points used in the search.

$[\bar{\eta}]_{DV,i}$ is the local intrinsic viscosity determined by DV and DRI at ith-specific retention volume. It is a function of the transport time.

$[\eta]_{cal,i}$ is the intrinsic viscosity at ith-specific retention volume, obtained from the cubic polynomial or the least square cubic spline fit to narrow standard calibration.

$s_{\eta sp,i}^2$ is the error variance estimate associated with $\eta_{sp,i}$, the specific viscosity at ith-specific retention volume, and $s_{[\eta]cal,i}^2$ is the error variance estimate of $[\eta]_{cal,i}$.

$s_{[\eta]cal,i}^2$ is estimated from the linear regression of the polynomial.

APPENDIX II

Nomenclature

o	concentration of polymer in the eluent
o_i	concentration of polymer in the eluent at ith-specific retention volume
DRI	differential refractive index detector
DV	differential viscometer

K	LALLS's optical constant
LALLS	low-angle laser light scattering photometer
$M_{cal,i}$	molecular weight obtained from narrow standard calibration at ith-specific retention volume
m_{DV}	total mass of polymer which has passed through DV in a run
M_i	local molecular weight at ith-specific retention volume
m_{LALLS}	total mass of polymer which has passed through LALLS in a run
$\bar{M}_n$	number average molecular weight
$\bar{M}_w$	weight average molecular weight
$\bar{M}_{w,i}$	local molecular weight determined by LALLS and DRI at ith-specific retention volume
$\bar{M}_z$	z average molecular weight
n	number of data points used in a numerical search
$O_1(t_{DRI\text{-}LALLS})$	objective function for the determination of $t_{DRI\text{-}LALLS}$
$O_2(t_{DRI\text{-}DV})$	objective function for the determination of $t_{DRI\text{-}DV}$
Q	total volumetric flow rate passing through both the LALLS and DV branches
Q_{DRI}	volumetric flow rate passing through DRI
Q_{DV}	volumetric flow rate passing through DV
Q_{LALLS}	volumetric flow rate passing through LALLS
R_θ	Excess Rayleigh scattering measured by LALLS
$R_{\theta,i}$	Excess Rayleigh scattering measured by LALLS at ith-specific retention volume
SEC	size exclusion chromatograph

$s_{cal,i}^2$	error variance estimate associated with $M_{cal,i}$
s_{Ci}^2	error variance estimate associated with c_i
s_i^2	estimate of the total error variance at ith-specific retention volume
$s_{lalls,i}^2$	error variance estimate associated with $\bar{M}_{w,i}$
$s_{R\theta,i}^2$	error variance estimate of $R_{\theta,i}$
$s_{[\eta]cal,i}^2$	error variance estimate of $[\eta]_{cal,i}$
$s_{\eta sp,i}^2$	error variance estimate associated with $\eta_{sp,i}$
t_{DET}	detection time
t_{DRI}	detection time of DRI
$t_{DRI\text{-}DET}$	interdetector transport time
$t_{DRI\text{-}DV}$	interdetector transport time between DV and DRI
$t_{DRI\text{-}LALLS}$	interdetector transport time between LALLS and DRI
v	retention volume
V_{DRI}	mobile phase volume measured from the point at which the flow is split to DRI
V_{DV}	mobile phase volumes measured from the point at which the flow is split to DV
V_{LALLS}	mobile phase volume measured from the point at which the flow is split to LALLS
W_N	normalized DRI response at each retention time
Δt_{DRI}	detection time increment for data collected for DRI
Δt_{DV}	detection time increment for data collected for DV
Δt_{LALLS}	detection time increment for data collected for LALLS
Δv	product of Q and Δt_{DRI}

Δv_{DET}	detection volume increment
Δv_{DV}	product of Q_{DV} and Δt_{DV}
Δv_{LALLS}	product of Q_{LALLS} and Δt_{LALLS}
$[\bar{\eta}]$	whole polymer intrinsic viscosity
$[\eta]_{cal,i}$	intrinsic viscosity obtained from narrow standard calibration at ith-specific retention volume
$[\bar{\eta}]_{DV,i}$	local intrinsic viscosity determined by DV and DRI at ith-specific retention volume
$[\bar{\eta}]_i$	local intrinsic viscosity at ith-specific retention volume
η_{sp}	specific viscosity measured by DV
$\eta_{sp,i}$	specific viscosity measured by DV at ith-specific retention volume